Appl. Phys. A 80, 597–600 (2005)
DOI: 10.1007/s00339-003-2236-z

Applied Physics A
Materials Science & Processing

F. JING
H. TONG
L. KONG
C. WANG✉

Electroless gold deposition on silicon(100) wafer based on a seed layer of silver

Department of Chemistry, Lanzhou University, Lanzhou 730000, P.R. China

Received: 30 January 2003 /Accepted: 20 May 2003
Published online: 25 July 2003 • **© Springer-Verlag 2003**

ABSTRACT This article describes a method of electroless gold deposition on a Si(100) wafer having a silver surface as seed layer. The seed layer was firstly deposited onto the surface of an etched wafer in an acidic solution of 0.005 mol/L $AgNO_3 + 0.06$ mol/L HF. The electroless gold deposition is performed by immersing the Ag-activated wafer in an electroless bath with a composition of 1.27×10^{-3} mol/L $[AuCl_4]^- +$ 2.00×10^{-2} mol/L $NaH_2PO_2 + 8.32 \times 10^{-2}$ mol/L $NH_2CH_2CH_2NH_2$ (pH = 9.0–9.5). The bath temperature is 50–70 °C. The morphology of the seed layer and the gold film were characterized by atomic force microscopy (AFM) and X-ray photoelectron spectroscopy (XPS).

PACS 82.45.Mp; 81.15.Pq; 81.10.Dn

1 Introduction

The technology of electroless metal deposition on a silicon wafer has been widely applied to the manufacture of ultra-large-scale integration (ULSI) and computer engineering [1] because of its suitability for depositing uniform films on the wafer. In addition, it is advantageous since it requires no external current or elaborate equipment.

In recent years, copper (Cu) has been proposed as an alternative material to aluminum to address the need for metallic thin films with low electrical resistivity and high electromigration resistance [2, 3]. However copper diffuses through silicon and forms electrically active deep levels in the energy band gap of silicon, degrading the electrical performance of the device [4, 5]. In addition, copper does not adhere to silicon oxide and does not form a self-passivating oxide for corrosion control [6, 7].

Gold films are used to produce solderable, gluable and bondable surfaces on circuit boards and other electronic components and to produce electric contacts. The films were originally produced by electrolytic methods. However, there are some disadvantages to the methods. In many cases, gold can not be deposited electrolytically at all, because surfaces that are electrically insulated from one another must be gold plated [8]. Therefore electroless methods have been developed. The past works provided methods for forming a seed layer to electroless gold deposition, such as electrolytic or electroless deposition of palladium [9–11], nickel or nickel alloy [12] and Co-W-P [13] films. The present work describes a new method of using silver as the seed layer for electroless gold deposition. In comparison to other metals, Ag does not diffuse to the inside of the silicon wafer so that it can play a role for preventing the possible diffusion of gold. On the other hand, gold is more stable in the atmosphere, the resistivities of gold and silver are 2.35 μ Ω cm and 1.61 μ Ω cm and its conductivity is only inferior to those of silver and copper.

There are some reports on electroless gold deposition using gold(I) cyanide compounds [12, 14, 15], for the reason that gold cyanide is stable in alkali solution and is easily obtained. But cyanide compounds have a heavy toxicity; thus they are not convenient in experiments and do great harm to the environment. In this method we use the complex ions of $[AuCl_4]^-$ as the main salt for electroless gold deposition. Compared with other cyano complexes of gold (sodium gold cyanide, potassium gold cyanide, ammonium gold cyanide), $[AuCl_4]^-$ has little toxicity. So it is safer to the environment. The plating bath containing $[AuCl_4]^-$ is more stable when a stabilizer (ethylenediamine) is added and the pH range is 9 – 9.5.

For the purpose of ensuring the elemental composition of the film and to elucidate the difference between the gold and silver films, atomic force microscopy (AFM) and X-ray photoelectron spectroscopy (XPS) analyses of the samples were employed.

2 Experimental

2.1 *Instrumentation*

A P47-SPM-MDT atomic force microscope (Solver) with tapping mode and a PHI-5702 multifunctional X-ray photoelectron spectroscope (USA, the instrument was calibrated by the measurement of the XPS spectrum of C 1*s* at 284.6-eV binding energy with a Mg K_α excitation source; the accuracy of band-energy measurements is ±0.3 eV) were used.

2.2 *Chemicals and materials*

1.27×10^{-2} mol/L $[AuCl_4]^-$stock solution was prepared by dissolving 0.0500 g gold (99.9999%) in 4 ml

✉ Fax: +86-931/891-2582, E-mail: wangcm@lzu.edu.ch

concentrated nitro-hydrochloric (1 : 3) acid in a temperature-controlled water bath at 95 °C. The corresponding dissolving reaction is as follows:

$$Au + 4HCl + HNO_3 = HAuCl_4 + NO + 2H_2O \quad (1)$$

Then 0.05 g KCl and 42 ml HCl (36%) were added. The solution was finally diluted to 100 ml with chlorine-saturated water. 0.1000 mol/L $AgNO_3$ stock solution was prepared by dissolving 4.2470 g $AgNO_3$ in 250 ml water in a brown flask. The chemicals HCl (36%), H_2O_2 (31%), HF (40%), NH_4OH (25%), $NH_2CH_2CH_2NH_2$ (99.0%), KOH, NH_4F and NaH_2PO_2 were all of analytical-reagent grade. Milli-Q water (Millipore 18.2 M Ω cm^{-1}) was used throughout. A (100) *p*-type silicon wafer with resistivity of 15–20 Ω cm^{-1} and thickness of 650 + 25 μm (Beijing Youyan Silicon Villa Semiconductor) was used.

2.3 *Wafer treatment*

The silicon wafer was cut to produce square samples with 1-cm^2 surface area. Firstly the wafer was cleaned in an ultrasonic cleaner in absolute alcohol for 10 min. Then the wafer was immersed in a hot solution of $H_2O_2 : NH_4OH : H_2O$ (1 : 1 : 5) for 10 min and next in another hot solution of $H_2O_2 : HCl : H_2O$ (1 : 1 : 6) for 10 min to remove possible contamination. Finally the wafer was treated in a solution of 10 ml HF (40%) + 100 ml NH_4F (40 g NH_4F in 100 ml H_2O) for 2 min at room temperature to remove silicon native oxide. The wafer was rinsed with water after each cleaning step.

2.4 *The preparation of silver seed layer*

The preparation of the silver seed layer (Ag-activated wafer) was performed by immersing the treated silicon wafer in a solution of 0.005 mol/L $AgNO_3$ + 0.06 mol/L HF for 5 s at room temperature.

2.5 *The electroless deposition of gold film*

The electroless deposition of the gold film was performed by immersing the Ag-activated wafer in an electroless gold bath at 65 °C for different times. The general composition of the bath was 1.27×10^{-3} mol/L $[AuCl_4]^-$ + 2.00×10^{-2} mol/L NaH_2PO_2 + 8.32×10^{-2} mol/L $NH_2CH_2CH_2NH_2$ (pH = 9.0–9.5).

3 Results and discussion

3.1 *The AFM analysis of the silicon(100) wafer with different surfaces*

The two-dimensional (2D) and three-dimensional (3D) AFM images of blank *p*-type silicon(100) are shown in Fig. 1, left and right, respectively. As can be seen from the figure, the silicon itself is flat enough, so the signal was almost at noise level. Because the wafer underwent an initial oxide-removal etching in the solution of 10 ml HF (40%) + 100 ml NH_4F, the images represent the surfaces of a hydrogen-terminated silicon substrate [16].

Figure 2 shows the AFM images of Ag seed layers on the silicon(100) wafer. The distribution of the Ag particles is very dense and the film is very uniform. The deposited particles have a size of about 50 nm and are randomly distributed on the surfaces. It is observed that the particles are composed of small Ag nuclei. The average surface roughness (R_a) of the Ag-activated wafer is 1.878 nm as measured by AFM. By comparing Fig. 1 and Fig. 2, we can conclude that a fine thin silver layer is deposited on the surface of the silicon wafer.

Figure 3 shows the AFM images of electrolessly deposited Au films on an Ag-activated silicon wafer. The deposited

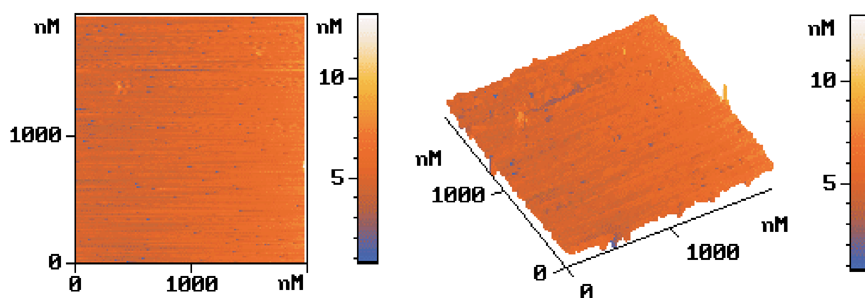

FIGURE 1 AFM images of silicon wafer after cleaning treatment

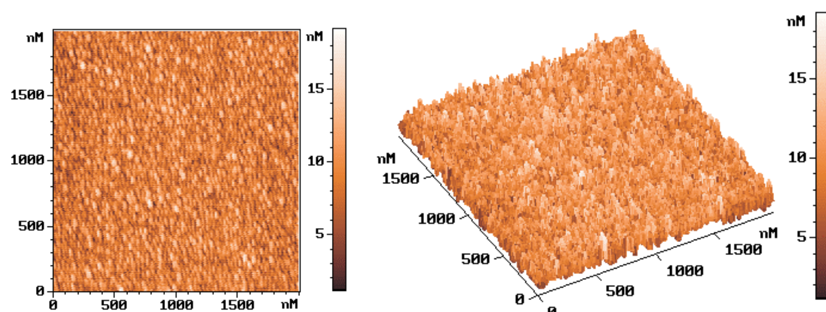

FIGURE 2 AFM images of the Ag seed layer

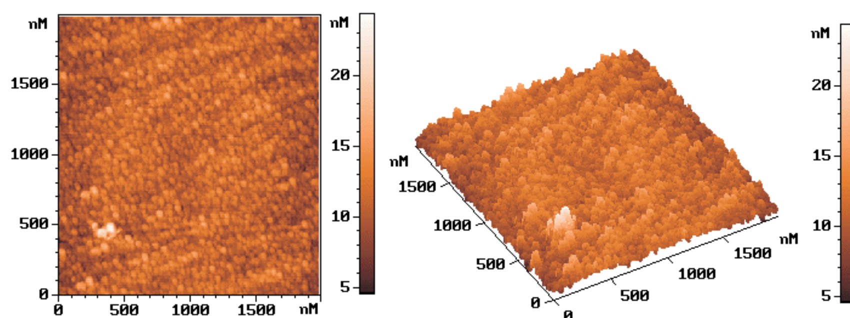

FIGURE 3 AFM images of electrolessly deposited gold film on the silver seed layer. Bath temperature: 65 °C. Deposition time: 30 s

Au surface shows a periodic parallel and row-like structure. Many small pellets in each row are clearly observed and have an average diameter about 80 nm, and they are organized in a two-dimensional pattern. The measured R_a is 1.378 nm. However, because of the discontinuity of the rows, the macrostructure of the Au layer is more like an island growth. By comparing Fig. 2 and Fig. 3, the Au layer shows a different growth pattern to that of the Ag seed layer. In other words, the Au growth pattern is not influenced by the deposited Ag layer.

According to the theory of hard–soft acids and bases [17], hard acids prefer to bind to hard bases and soft acids prefer to bind to soft bases. For a given metal ion, the stability of complexes with different ligands follows the theory above. By comparison, Cl^- is a relatively softer base than ethylenediamine. As a soft acid, Au^{3+} forms a more stable complex with Cl^- ions (the logarithm of the $AuCl_4^-$ stability constant is $\log\beta = 26$) [18]. So $AuCl_4^-$ complex ions are stable in the electroless Au deposition solution of 1.27×10^{-3} mol/L $[AuCl_4]^- + 2.00 \times 10^{-2}$ mol/L NaH_2PO_2 $+ 8.32 \times 10^{-2}$ mol/L $NH_2CH_2CH_2NH_2$ (pH = 9.0–9.5). For the deposition of metallic gold on the Ag seed layer, the following electrochemical reactions are considered:

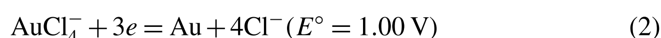

$$AuCl_4^- + 3e = Au + 4Cl^- (E^\circ = 1.00\ V) \quad (2)$$

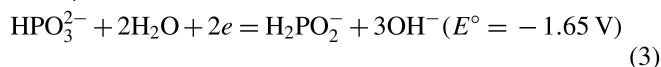

$$HPO_3^{2-} + 2H_2O + 2e = H_2PO_2^- + 3OH^- (E^\circ = -1.65\ V) \quad (3)$$

where E° is the standard reduction potential. Therefore, we could infer that the redox reaction between $AuCl_4^-$ and $H_2PO_2^-$ as indicated in (4) below is thermodynamically possible by comparing the E° value to those of reactions (2) and (3). The electrons required for the gold deposition are supplied by the oxidation of $H_2PO_2^-$.

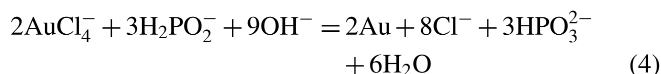

$$2AuCl_4^- + 3H_2PO_2^- + 9OH^- = 2Au + 8Cl^- + 3HPO_3^{2-} + 6H_2O \quad (4)$$

It is found that ethylenediamine plays an important role as the stabilizer in the electroless gold bath. The homogeneous bath can be kept for one week with the existence of this stabilizer. KOH was used to adjust the pH of the bath. When the pH is below 9, the stability of the bath is not satisfactory. At higher pH, more than 9.5, the deposition speed becomes slow. The temperature of the bath solution obviously affects the Au deposition speed. The speed of electroless Au deposition is lower when the bath temperature is below 50 °C. From this temperature, the Au deposition speed increases with increasing temperature. However, when the temperature is higher than 80 °C the surface roughness degree of the Au film increases.

3.2 *XPS analysis of the silicon(100) wafer with different surfaces*

The XPS spectrum of the silver seed layer on a silicon wafer is shown in Fig. 4. The spectrum confirmed that the deposited grains were pure Ag phase. The XPS Ag 3*d* core energy peaks of the Ag-activated substrates were located at 374.48 eV and 368.4 eV, respectively. No other metal elements were found from the XPS spectrum.

Figure 5 shows the XPS spectra for the sample corresponding to the gold film on a silver seed layer. The Ag 3*d* core energy peaks are still observed as shown in Fig. 5a. But a small shift of the peaks from 374.48 eV and 368.4 eV (Fig. 4) to 373.76 eV and 367.79 eV is found. The presence of gold was detected for the sample. The energy peaks of the Au 4*f* core appeared at 83.69 eV and 87.47 eV (Fig. 5b). So we can confirm that gold is deposited on the silver seed layer. This conclusion is strongly supported by the AFM results as shown in Figs. 2 and 3.

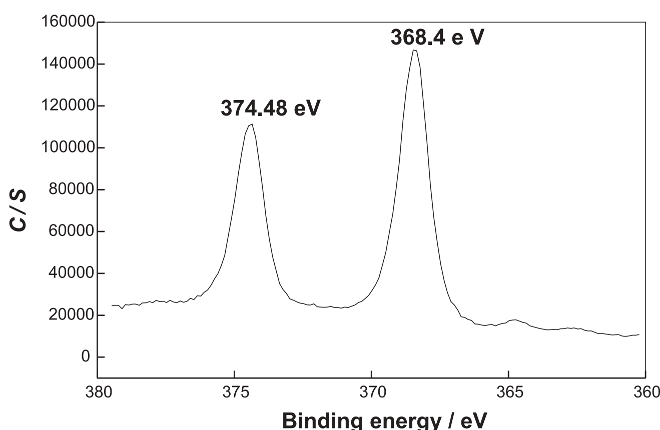

FIGURE 4 XPS spectrum for silver seed layer on silicon wafer

4 Conclusions

Silver seed and gold layers were deposited by using the electroless method. A *p*-Si(100) wafer was used as the substrate. The solution of 0.005 mol/L $AgNO_3$ +

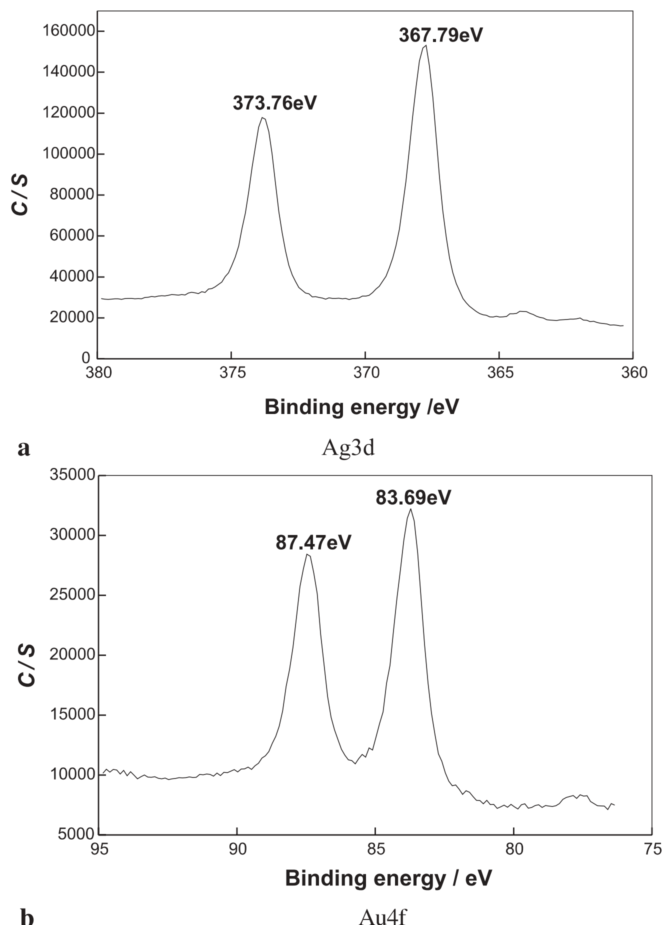

FIGURE 5 The XPS spectra of electrolessly deposited gold film on the silver seed layer

0.06 mol/L HF was taken as the electroless bath for the seed layer and the solution of 1.27×10^{-3} mol/L $[AuCl_4]^-$ + 2.00×10^{-2} mol/L NaH_2PO_2 + 8.32×10^{-2} mol/L $NH_2CH_2CH_2NH_2$ (pH = 9.0–9.5) as the electroless bath for the gold layer. The film morphology of both layers was investigated by AFM and XPS. The Au layer shows a different growth pattern to that of the Ag seed layer.

ACKNOWLEDGEMENTS This work was supported by the National Natural Science Foundation of China (Grant No. 20073017).

REFERENCES

1. V.M. Dubin, Y. Shacham-Diamand, B. Zhao, P.K. Vasudev, C.H. Ting: J. Electrochem. Soc. **144**, 898 (1997)
2. J.S.H. Cho, H. Kang, S.S. Wong, Y. Shacham-Diamand: MRS Bull. **18**, 31 (1993)
3. L. Magagnin, R. Maboudian, C. Carrao: Electrochem. Solid State Lett. **4**, C5 (2001)
4. Y. Shacham-Diamand, A. Dedhia, D. Hoffstetter, W.G. Oldham: J. Electrochem. Soc. **140**, 2427 (1993)
5. G. Raghavan, C. Chiang, P.B. Anders, S.M. Tzeng, R. Villasol, G. Bai, M. Bohr, D.B. Fraser: Thin Solid Films **262**, 168 (1995)
6. J. Li, Y. Shacham-Diamand, J.W. Mayer: Mater. Sci. **9**, 1 (1992)
7. A. Kohn, M. Eizenberg, Y. Shacham-Diamand. Y. Sverdlov: Mater. Sci. Eng. A **302**, 18 (2001)
8. P. Backus, H. Mahlkow, C. Wunderlich: US Patent No. 6 336 962 (2002)
9. A. Inherg, L. Zhu, G. Hirschberg, A. Gladkikh, N. Croiyoru, Y. Shacham-Diamand, E. Gileadi: J. Electrochem. Soc. **148**, C784 (2001)
10. Y. Shacham-Diamand, A. Inberg, Y. Sverdlov, N. Croitoru: J. Electrochem. Soc. **147**, 3345 (2000)
11. G.L. Ballard, R.D. Edwards, J.G. Gaudiello, V.R. Markovich: US Patent No. 6 383 617 (2002)
12. M. Kato, J. Sato, H. Otani, T. Homma, Y. Okinaka, T. Osaka, O. Yoshioka: J. Electrochem. Soc. **149**, C164 (2002)
13. C.J. Sambucetti, J.M. Rubino, D.C. Edelstein, J.C. Cabral, G.F. Walker, J.G. Gaudiello, H.S. Wildman: US Patent No. 6 323 128 (2001)
14. T. Osaka, T. Misato, J. Sato, H. Akiya, T. Homma, M. Kato, Y. Okinaka, O. Yoshioka: J. Electrochem. Soc. **147**, 1059 (2000)
15. S. Warren, A. Reitzle, A. Kazimirov, J.C. Ziegler, O. Bunk, L.X. Cao, F.U. Renner, D.M. Kolb, M.J. Bedzyk, J. Zegenhagen: Surf. Sci. **496**, 287 (2002)
16. S.W. Lim, R.T. Mo, P.A. Pianetta, C.E.D. Chidsey: J. Electrochem. Soc. **148**, C16 (2001)
17. J.E. Huheey: *Inorganic Chemistry,* 2nd edn. (Harper and Row, New York 1978) p. 276
18. Y. Zhu: *A Handbook of Electrochemical Data* (Hunan Science and Technology Press 1984) p. 14